THE D+D FUSION REACTIONS AT VERY LOW ENERGIES

H. PAETZ GEN. SCHIECK

Institut für Kernphysik, Universität Köln, Zülpicher Str. 77, 5000 Köln 41, Germany

ABSTRACT: The D+D fusion reactions are among the oldest nuclear reactions studied. Due to their complex nature the reaction mechanism is still under intensive investigation. Polarization observables play an important role. Applications such as possible neutron-lean "polarized fusion" lead to new theoretical and experimental efforts to study these reactions at very low energies (e.g. 28 keV).

1. INTRODUCTION

The $D(d,n)^3He$- and $D(d,p)^3H$ fusion reactions are of special interest for several reasons. One is the nuclear physics of few-nucleon systems, another are fusion energy applications.

They belong to the earliest nuclear reactions investigated both theoretically [1] and experimentally [2]. Their large cross sections even at very low energy, their relation to states in ^4He - the A=4 system being the lightest nuclear system known to have excited-state structure - and their special symmetry properties (identical particles in the entrance channel) have made them attractive. They display some unusual features, such as contributions from P waves even at c.m. energies as low as 15 keV (seen directly in cross-section anisotropies and in substantial vector analyzing powers, which are due mainly to S- and P-wave interference) and even from D waves above c.m. energies of 50 keV.

All analyses showed that the reaction mechanism of the two D+D fusion reactions even at very low energies is very complex and requires participation of all possible transitions. Therefore the disentanglement of the relative strength of these is a difficult task and requires many independent (i.e. mostly polarization) experiments. Experimentally the situation is far away from "complete" in the sense that more independent measurements at all energies than the necessary minimum required by the structure of the transition matrix had been performed, as is the case for the nucleon-nucleon interaction.

The four-nucleon system as the smallest few-nucleon system having excited states is also of considerable theoretical interest. Though the relevant equations have existed for a long time [3] only recently results of microscopic (i.e. based on realistic nucleon-nucleon potential input) 4-body (Faddeev) calculations have been presented [4]. Before, different approximative approaches have been taken, ranging from a simple potential model [5] to DWBA [6] and refined-resonating-group (RRGM) ,see e.g. [7], calculatons.

As to the potential fusion-energy application of polarized D+D fusion reactions a renewed interest in general low-energy studies of these reactions was kindled by the proposal of a "neutron lean" fusion reactor based on the $^3He(\vec{d},p)^4He$ reaction. Such a potential reactor will be aneutronic only if the $D(d,n)^3He$ reaction rate could be substantially suppressed. Provided quintet states (with the spins of both reacting deuterons aligned parallel) would not contribute in the D(d,n) reaction, then the use of deuterons polarized along the direction of the plasma confining magnetic field would lead to a suppressed neutron production rate and, in conjunction with ^3He nuclei as well, to a possible rate increase (or lower ignition limit) for the $^3He(d,p)^4He$ fusion in analogy to the $^3H(d,n)^4He$ case [8,9].

Therefore, the magnitude of the contribution (or suppression) of quintet states in the two reactions and possible channel spin transitions with $\Delta S = 1$ (such as quintet-triplet or $\Delta S = 2$ (quintet-singlet transitions) are of special interest. Contributions from these quintet states have been excluded in the past by an argument based on the Pauli principle. This argument may be considered very weak because of the extremely large interaction radius of two deuterons. In fact, a careful analysis of the data of the D(d,p) reaction at 290 keV in terms of partial waves [10] seemed to show a certain amount of quintet-state suppression. A later analysis of data by the same group and comparison with all other available data in the energy range below 485 keV showed in addition that transitions from the quintet-S state of the D(d,n) branch appear to be hindered relative to the D(d,p) branch [11]. In contrast to this finding a multi-channel R-matrix analysis of all available data of the four-nucleon system by Hale [7] yielded no quintet suppression. Theoretical approaches, on the other hand, differed widely in their predicitions. Defining the ratio of the integrated S=2 partial cross section (i.e. with both deuterons polarized in parallel) to the unpolarized integrated cross section as quintet suppression factor QSF, the RRGM calculation predicted QSF ~ 0.9 (almost no suppression) at $E_{c.m.} = 25$ keV whereas the DWBA calculation [6]

found a constant QSF = 0.08. Strong objections have been raised against the DWBA approach together with arguments for strong quintet state contributions via the D state of the deuteron [7,12]. The question of quintet states has to be decided by experiment, preferable by direct measurement of the spin-correlation cross sections, which, however, has not been possible so far. A direct matrix-element fit by Lemaitre et al. [13] of all available data of both D+D fusion reactions below 500 keV even yielded some quintet state enhancement calculated from the values of all 16 matrix elements resulting from this analysis (see below).

Though many data at low energies (< 1 MeV), including polarization data, exist, the data situation is not very satisfactory. E.g. sets of analyzing power data of different groups scatter widely outside the errors and even unpolarized cross sections of different labs. are not in good agreement. $D(d,n)^3He$ data are scarce and this is true especially at very low energies < 100 keV. Additional data at very low energies are highly desirable for several reasons : the matrix element analysis can be made much more reliable by fixing the low energy trend of the data and the measurements would be made at energies, at which future fusion reactors would probably work. In addition : since the D+D reactions are the only ones sensitive to vector polarization at such low energies the accurate measurement of the vector analyzing powers A_y can be useful for low-energy polarimeters to be used in conjunction with polarized sources or jet targets at accelerators with recirculating beams (LEAR, COSY).

These arguments prompted several laboratories to start cross-section and analyzing-power measurements [14,15] and even to build dedicated low-energy polarized beam facilities such as at the TUNL laboratory. At Cologne a complete set of analzying powers for both the $D(\vec{d},n)^3He$ and $D(\vec{d},p)^3H$ reactions at $E_{lab.} = 28 \pm 3$ keV was obtained and included in the matrix-element analysis. Both will be discussed below.

2. FORMAL DESCRIPTION OF THE D+D REACTIONS

Following Ad'yasevich [16] we define the 16 transitions, necessary to describe the D+D fusion reactions at low energies in the following way :

Table 1

DEFINITION OF THE MATRIX ELEMENTS $T_{\beta\alpha}(E)$:

$\langle {}^{2S_\alpha+1}\ell_{\alpha_J} | J^\pi | {}^{2S_\beta+1}\ell_{\beta_J} \rangle$, α for the entrance channel, β for the exit channel, in an angular momentum basis :

	$S_\alpha = 0$ Singlet	$S_\alpha = 1$ Triplet	$S_\alpha = 2$ Quintet
$\ell_\alpha = 0$	$\alpha_0 = \langle {}^1S_0 \mid 0^+ \mid {}^1S_0 \rangle$		$\gamma_1 = \langle {}^5S_2 \mid 2^+ \mid {}^1D_2 \rangle$ $\delta_1 = \langle {}^5S_2 \mid 2^+ \mid {}^3D_2 \rangle$
$\ell_\alpha = 1$		$\alpha_{10} = \langle {}^3P_0 \mid 0^- \mid {}^3P_0 \rangle$ $\beta_{11} = \langle {}^3P_1 \mid 1^- \mid {}^1P_1 \rangle$ $\alpha_{11} = \langle {}^3P_1 \mid 1^- \mid {}^3P_1 \rangle$ $\alpha_{12} = \langle {}^3P_2 \mid 2^- \mid {}^3P_2 \rangle$ $\alpha_3 = \langle {}^3P_2 \mid 2^- \mid {}^3F_2 \rangle$	
$\ell_\alpha = 2$	$\alpha_2 = \langle {}^1D_2 \mid 2^+ \mid {}^1D_2 \rangle$ $\beta_2 = \langle {}^1D_2 \mid 2^+ \mid {}^3D_2 \rangle$		$\gamma_2 = \langle {}^5D_0 \mid 0^+ \mid {}^1S_0 \rangle$ $\gamma_3 = \langle {}^5D_2 \mid 2^+ \mid {}^1D_2 \rangle$ $\delta_2 = \langle {}^5D_1 \mid 1^+ \mid {}^3S_1 \rangle$ $\delta_3 = \langle {}^5D_1 \mid 1^+ \mid {}^3D_1 \rangle$ $\delta_4 = \langle {}^5D_3 \mid 3^+ \mid {}^3D_3 \rangle$ $\delta_5 = \langle {}^5D_2 \mid 2^+ \mid {}^3D_2 \rangle$

In the early potential model description of the D+D reactions [5,17] it was assumed that the energy dependence of the transition amplitudes is entirely governed by Coulomb and centrifugal barriers in the entrance channel. Therefore like in many early approaches (e. g. [16,18]) we consider the transition amplitudes

$T_{\beta\alpha}(E)$ to factorize like

$$T_{\beta\alpha}(E) = C_{\ell_\alpha}(E) \; \hat{T}_{\beta\alpha} \tag{1}$$

into an energy-dependent penetrability factor and an "internal" energy-independent ampitude $\hat{T}_{\beta\alpha}$ with :

$$C_{\ell_\alpha}(E) = \sqrt{P_{\ell_\alpha}(E)} \; \exp[i(\delta_{\ell_\alpha} + \varphi_{\ell_\alpha})] \tag{2}$$

$$P_{\ell_\alpha}(E) = \frac{1}{F_{\ell_\alpha}(E)^2 + G_{\ell_\alpha}(E)^2} \tag{3}$$

Here F_{ℓ_α} and G_{ℓ_α} are the regular / irregular solutions of the Schrödinger equation for the scattering of two charged particles which approach to a distance of R. The phases

$$\delta_{\ell_\alpha} \text{ and } \varphi_{\ell_\alpha}$$

are well-known:

$$\begin{aligned} \delta_{\ell_\alpha} &= -\arctan(F_{\ell_\alpha} / G_{\ell_\alpha}) \\ \varphi_{\ell_\alpha} &= \arg \Gamma(\ell_\alpha + 1 + i\eta) \end{aligned} \tag{4}$$

The condition that the $\hat{T}_{\beta\alpha}$ are constant in the energy range of interest can only be fulfilled in a limited range of low energies, however.

In a two-particle reaction A(a,b)B where, in the entrance channel, each particle may be polarized, or, in the exit channel, the polarization of each particle may be measured , the tensor moments of the exit channel β (in spherical notation) as functions of the tensor moments of the entrance channel α may be written in the most general way as

$$t^{\beta}_{k_B q_B, k_b q_b} = \langle \tau_{k_B q_B} \tau_{k_B q_B} \rangle = [\mathrm{Tr}\,(\rho_\beta)]^{-1}\, \mathrm{Tr}(T \rho_A \rho_a T^{+} \tau_{k_B q_B} \tau_{k_b q_b}) \tag{5}$$
$$= \sigma_0(\vartheta)/\sigma_{pol}(\vartheta) \sum_{\substack{k_A q_A \\ k_a q_a}} t_{k_A q_A, k_a q_a} \Xi^{k_B q_B, k_b q_b}_{k_A q_A, k_a q_a}(k_\beta, k_\alpha)$$

The τ_{kq} are (spherical) spin operators, the ρ spin density operators (matrices). All information concerning the nuclear dynamics as well as the reaction geometry is contained in the generalized analyzing powers

$$\Xi^{k_B q_B, k_b q_b}_{k_A q_A, k_a q_a}(k_\beta, k_\alpha) = \frac{\mathrm{Tr}\left\{ T\, \tau^{+}_{k_A q_A} \tau^{+}_{k_a q_a} T^{+}\, \tau_{k_B q_B} \tau_{k_b q_b} \right\}}{\mathrm{Tr}(T\, T^{+})} \tag{6}$$

The reaction amplitudes $T_i \equiv T_{\beta\alpha}$ and equation (5) are often represented in a partial wave expansion (i.e. in an angular momentum basis). A general formula for this expansion has been given by Welton [19] and extended to charged particles by Heiss [20]. It shows how to perform Legendre expansions of all possible observables, e.g. those relevant for the D+D fusion reactions. Each Legendre expansion coefficient of each observable can then be related to products of transition matrix elements by an expansion using the Welton formalism.

A computer code FATSON/TUFX [21], originally written to perform the necessary angular momentum algebra of the Welton formula, was changed to obey the Madison convention and was then extended to charged particles and also identical particles in the entrance channel. It was used to determine numerically the coefficients of the expansion of the Legendre coefficients of all D+D observables in terms of products of the transition matrix elements $T_{\beta\alpha}$. All similar expansions with coefficients published in the literature were thus shown to contain at least some errors, including those of Ad'yasevich et al. who performed the most comprehensive analysis of D+D data so far [16].

Using these coefficients a fitting routine for the Legendre expansion coefficients in terms of the 16 complex "internal" transition matrix elements $\hat{T}$ (corresponding to 31 unknowns due to one arbitrary phase) was written [13] and

applied to existing low-energy data sets of the D+D fusion reactions. It was possible to achieve a satisfactory fit and results for all transitions. Conclusions about the strength of the quintet state transitions and any other observable of both reactions were possible.

3. EXPERIMENTAL PROGRAM

As explained above, analyzing power measurements for the D+D fusion reactions have been performed at $E_{lab.}$ = 28 ± 3 keV, using the Cologne polarized ion source LASCO high voltage platform as accelerator.

3.1. General experimental problems at very low energies

In measurements of deuteron analyzing powers at extremely low energies one has to deal with a number of specific problems :

- For the vector polarization of the beam there exists no polarization analyzing reaction (due to normally pure S-wave contributions only) except for the D+D reactions proper. The vector polarization of the beam therefore has to be measured after acceleration to higher energies where a known analyzer exists (or has to be inferred from the measured tensor polarization using known properties of the source of polarized ions; this will normally introduce appreciable uncertainties into the results and does not work too well for Lambshift sources). If the accelerator used can bridge the energy gap from the low to the high energy range, then successive intercalibration runs at different energies are possible, which avoids possible depolarization, but increases the errors. In the other case one has to make sure that depolarization is insignificant.
- For the tensor polarization the $^3H(d,\alpha)n$ reaction, which proceeds via S waves and which is almost entirely governed by the broad $J^\pi = 3/2^+$ resonance at E_d=107 keV, constitutes a good analyzer with known analyzing power in the entire energy range below 100 keV. A conjectured small contribution from $J^\pi=1/2^+$ would introduce some (< 5%) uncertainty in the results. However, recent RGM calculations [22] showed no such state of relevance to low energy polarization measurements. Another method would be the same as that used for the vector polarization measurement, namely to measure the polarization after acceleration to

higher energies by the tandem VdG accelerator and using the $^3He(d,p)^4He$ reaction at $\Theta = 0^o$.

- Due to charge exchanges in the target the measurement of the true beam current becomes difficult. Different methods to overcome this problem have been developed, e. g. calorimetric or pyro-electric methods. For the vector analyzing power measurement with a symmetric detector pair the left-right asymmetry can be obtained without a beam charge normalization. This is not possible for the tensor analyzing powers where alternating polarized und unpolarized runs have to be taken. In principle, absolute current normalization is not needed. It is sufficient to have a method which ensures equal amounts of charge in both runs. However, depending on the number of detectors used for one polar angle, for all effects except A_{zz} exact beam charge normalization would provide additional checks on the quality of the measurement ("CT factor", see below).
- Targets have to be very thin, though below the Bethe-Bloch maximum the energy loss decreases. Especially for the extreme forward and backward angles the definition of the target volume in a gas target becomes more uncertain and the use of entrance and exit foils prohibitive. Ideally a jet target such as in [16] could be used. However, due to differential pumping requirements this would be difficult to realize for the 4π geometry required for the tensor analyzing power measurements. Therefore solid targets, provided they can be made sufficiently thin and mechanically and thermally stable, are a good choice. In the tensor analyzing power measurements, thickness changes have to be monitored and, if possible, compensated ("CT factor").

3.2. Polarized beam and polarization measurement

The polarized deuteron beam was produced by the Cologne Lambshift source LASCO and accelerated into an ORTEC-600 scattering chamber (for the vector analyzing-power measurements) or a small 4π cube (for the tensor analyzing-power measurements), both downstream of the injector high voltage platform of the source. The Lambshift source allows the production of a purely vector and also of a purely tensor polarized deuteron beam. A Wien filter rotatable around the beam axis allows the orientation of the quantization axis into any desired

direction. Beam currents of several hundred nA from the source are routinely obtainable , so that reactions with rather low cross sections and coincidence experiments can be measured.

The vector polarization of the beam was measured by accelerating the beam in the usual way by the Cologne FN tandem accelerator into the vector polarimeter behind the 30" ORTEC-2800 scattering chamber. The ^{4}He(d,d) scattering at E_d= 14.0 MeV and Θ = 90°, where the analyzing power is known to be A_y = - 0.387 ± 0.006, was used as an analyzer. Since the left-right asymmetry in two symmetric detectors was measured, no charge normalization was necessary. The beam tensor polarization was similarly measured in a ^{3}He(d,p)^{4}He polarimater at 0° using a CsI scintillator and after stopping the deuteron beam in a biased Faraday cup in the high energy beam line. These measurements were performed at E_d = 10 MeV, where the tensor analyzing power is A_{zz} = - 1.417 ± 0.014 . The precision to which the polarization direction at all target locations can be set by the rotatable Wien filter on the source has been carefully checked by taking precession calibration curves and is estimated to < 1° for both the polar and azimuthal directions.

In order to ensure that no significant depolarization would occur the possible sources of such depolarization were studied. These are :

- Depolarization during the stripping process in the tandem terminal. This effect had been studied by Haeberli et al. [23] and found to be negligible for foil stripping .
- Inhomogeneous distribution of the polarization across the beam diameter together with varying degrees of interception of outer parts of the beam at diaphragms and slits. This effect was counteracted by using large diameter diaphragms and slits in the beam path and checked by comparing the measured beam polarization frequently for very different focussing conditions at the polarimeter. No significant differences were found.
- Depolarization in magnetic fields along the beam trajectory such as in quadrupole doublet lenses where a rotation of the quantization axis relative to the beam axis and a precession of the spins of the particles depending on different divergences of the particles, would cause the depolarization. These effects could be estimated with the formalism by [24] to cause a maximum depolarization of 0.6 %.

Therefore we concluded that in our experiment the depolarization effects could

be safely neglected. A vector polarization of p_z = 0.510 ± 0.005 was measured which was constant over the entire measurement within the error.

The maximum tensor polarization p_{zz} of the beam was -0.82, from which all three tensor polarization components for arbitrary directions of the quantization axis could be calculated with the known calibration of the Wien filter. A small remaining vector polarization of the beam which is caused by the necessity of maintaining a small magnetic field (< 1 Gs) at the argon charge exchange region in the source after the second quench process was estimated to be < 0.022 . With the methods chosen to measure the tensor analyzing powers this enters the results only to second order and therefore can be neglected .

3.3. Beam charge normalization

For the comparison of the beam charges for polarized and unpolarized runs several experimental schemes were investigated : e.g. a transmission Faraday cup ahead of the target consisting mainly of a fine tungsten mesh intercepting a constant fraction (~ 10 %) of the incident beam, here this constancy is essential and, due to effects from secondary electrons despite suppression, could not be maintained in a sufficiently stable way. Instead the beam was stopped in the target backing. The beam current onto the insulated target rod could then be measured after connecting a suitable positive bias voltage to it (about 30 V). Leakage currents from the target to ground via the current integrator due to this voltage were prevented by connecting the target ladder to the bias voltage through an insulated target rod.

3.4. Targets

Two different deuterated compounds were tested for thermal stability under beam bombardment : poly-ethylene $(CD_2)_n$ and para-polyphenyl DPP $(C_6D_5)_n$. The $(CD_2)_n$ targets were produced by evaporating the powder material onto a thin (5 to 9 $\mu g/cm^2$) carbon backing with an electron gun. Targets with thicknesses of 9 to 12 $\mu g/cm^2$ were tested and proved mechanically stable, but showed an unacceptable loss of thickness in the first 30 min. of irradiation with beam currents of 600 to 800 nA at an energy of 32 keV. The DPP targets by the Gießen group [25], of between 10 and 30 $\mu g/cm^2$ on thin carbon and aluminum backings, which were mechanically very sensitive, showed a weaker loss of

deuterium content under beam bombardment, depending on the backing thickness, and were therefore used here.

The thickness of the target backing was optimized to be just thick enough to stop the deuteron beam in order to allow especially the ^{3}He recoils to pass through the target backing with sufficient energy (> 400 keV) for being measurable above the noise in the spectra. This turned out to be very critical especially for angles near $\Theta = 90^\circ$ with four detectors where the target rod had to be introduced along the spatial diagonal of the target cube and at forward angles. The thickness optimization was done using an energy loss calculation program based on [26].

A serious problem of the experiment was the change of target thickness under beam bombardment caused by two competing processes. One is carbon growth due to dissociation of hydrocarbon molecules in the residual gas, the other is evaporation of target material by the heat deposited by the beam. The use of a LN_2 cold trap reduced the carbon buildup substantially, but not competely. Both processes lead to different nonlinear, but monotonic decreases of the count rate which, however, cannot be separated. The measurement of A_{zz} requires the knowledge of the ratio of the product of target thickness (factor T) and beam charge (factor C) between successive tensor polarized (p) and unpolarized (u) runs. The knowledge of C alone requires a functioning charge integration method. Thickness changes in the targets are compensated to first order by taking short runs in the sequence p-u-u-p and adding the p- and u-results. The CT factor was monitored during the A_{xz} and A_{xx}-A_{yy} runs by setting the polarization direction to $\beta = 54.7^\circ$ (where p_{zz}=0) and used to compute the A_{zz} data. Experimentally the value of CT was found to be close to 1, indicating good charge integration and target thickness monitoring.

The effects of the target changes due to the two processes on the average reaction energy in the target are different. Carbon buildup lowers the reaction energy whereas evaporation of target material leads to an increase. Since the relative contributions from both are not known we assumed equal contributions to the observed count rate decreases from both. On this basis the average reaction energy was calculated by taking the energy average over the target with the known integrated cross section $\sigma(E)$ as weighting factor. Its error was determined from the maximum possible variation of the energy due to target changes.

For a target of thickness 31.3 μg/cm the energy loss for an incident beam

of an energy of 34.5 keV was calculated to be 18.0 ± 3.0 keV. An average reaction energy of 28 ± 3 keV was obtained. Due to the strong energy dependence of this cross section the low-energy portion of reactions occuring nearer to the exit of the target foil do not contribute strongly to the reaction rate and to the energy average. Therefore this average energy is rather close to the incident energy, and its estimated error is rather small.

A typical count rate for the charged particles from the D + D reactions (with a detector solid angle of 24.8 msr and a beam current of 200 nA) using such a target was < 5 Hz.

3.5. Scattering chambers and detectors

The detectors used were silicon surface barrier detectors partly cooled to 15° C with solid angles up to 95 msr. The vector analyzing powers were measured with left-right symmetrical detector pairs in the reaction plane, the tensor analyzing powers with sets of for detectors for each polar angle in a 4π geometry. A liquid nitrogen trap was used to minimize carbon buildup on the target.

3.6. Measurement of the analyzing powers

In a coordinate system in agreement with the Madison convention the general Cartesian form of the cross section with polarized spin-1 particles can be written as :

$$(d\sigma/d\Omega)_{pol}(\Theta,\Phi)=(d\sigma/d\Omega)_0(\Theta)\{1+\frac{3}{2}p_y A_y(\Theta)+\frac{2}{3}p_{xz}A_{xz}(\Theta) +\frac{1}{6}(p_{xx}-p_{yy})[(A_{xx}(\Theta)-A_{yy}(\Theta)]+\frac{1}{2}p_{zz}A_{zz}(\Theta)\} \quad (7)$$

The beam-polarization components depend on the polar and azimuthal angles β and Φ of the spin quantization axis in the above coordinate system and on the maximum values p_z and p_{zz} When a detector arrangement of four detectors at the azimuthal angles $\Phi = 0°$(left), $\Phi = 180°$ (right), $\Phi = 90°$ (up) and $\Phi = 270°$ (down) for each polar angle Θ is chosen, then the ratios of the count rates with polarized (Z) and unpolarized (Z_0) beams as functions of cross-section ratios for each detector position L, R, U and D may be written :

$$\left.\begin{matrix} L \\ (R) \end{matrix}\right\} \equiv \left.\frac{Z}{Z_0}\right\}_{\substack{L \\ (R)}} = CT \cdot \left.\frac{d\sigma/d\Omega}{(d\sigma/d\Omega)_0}\right\}_{\substack{L \\ (R)}} = CT \left\{1 \begin{matrix} + \\ (-) \end{matrix} \frac{3}{2} p_z \sin\beta\, A_y \right. \tag{8}$$
$$\left. + \frac{1}{4} p_{zz} [(3\cos^2\beta - 1)\, A_{zz}(\theta) - \sin^2\beta [A_{xx}(\theta) - A_{yy}(\theta)]] \right\}$$

$$\left.\begin{matrix} U \\ (D) \end{matrix}\right\} \equiv \left.\frac{Z}{Z_0}\right\}_{\substack{U \\ (D)}} = CT \cdot \left.\frac{d\sigma/d\Omega}{(d\sigma/d\Omega)_0}\right\}_{\substack{U \\ (D)}} = CT \left\{1 + \frac{1}{4} p_{zz} [\begin{matrix} + \\ (-) \end{matrix} 4 \sin\beta \cos\beta\, A_{xz}(\theta) \right. \tag{9}$$
$$\left. + (3\cos^2\beta - 1)\, A_{zz}(\theta) + \sin^2\beta [A_{xx}(\theta) - A_{yy}(\theta)]] \right\}$$

$A_y(\theta)$ was obtained from a measurement of the asymmetry ε of the left and right count rates Z_L and Z_R with the purely vector-polarized beam and $\beta = \pm 90^o$ (Spin U/D)

$$A_y(\theta) = \frac{\varepsilon - 1}{\varepsilon + 1} \cdot \frac{2}{3 p_z} \quad \text{with} \quad \varepsilon = \left\{ \frac{Z_L^U Z_R^D}{Z_L^D Z_R^U} \right\}^{\frac{1}{2}} \tag{10}$$

For the tensor analyzing power measurements with the tensor polarized beam two different polarization directions were chosen. $A_{zz}(\theta)$ was measured with the quantization axis oriented longitudinally ($\beta = 0^o$) such that

$$A_{zz}(\theta) = [\frac{1}{CT}(U + D + L + R) - 4] / 2 p_{zz} \tag{11}$$

requiring a knowledge of the factor CT. The components $A_{xz}(\theta)$ and $A_{xx}(\theta) - A_{yy}(\theta)$ were measured, by setting $\beta = 54.7^o$, from the up-down asymmetry

$$A_{xz}(\Theta) = -\frac{3}{2\sqrt{2}} \frac{U-D}{U+D+R+L} \frac{1}{P_{zz}} \tag{12}$$

and from the left-up/right-down asymmetry

$$A_{xx}(\Theta) - A_{yy}(\Theta) = -\frac{3}{2} \frac{(L+R)-(U+D)}{U+D+R+L} \frac{1}{P_{zz}} \tag{13}$$

Though in these two cases the CT factor does not enter directly, it was chekked by taking the sum

$$CT = \frac{1}{4}(L+R+U+D) \tag{14}$$

which ideally should be equal to 1. The resulting CT values were used.

4. EXPERIMENTAL RESULTS

Fig. 1 shows the experimental results [27] of the four analyzing powers of the $D(\vec{d},n)^3He$ and $D(\vec{d},p)^3H$ reactions together with Legendre fits, the results from the multi-channel R-matrix parametrization by Hale [28] and from the new matrix-element fit . Fig. 2 gives the Legendre-fit results as error bands from the covariance matrix of the fit, in order to allow a comparison of the two mirror reactions. Differences between them are clearly visible.

5. LEGENDRE ANALYSIS

The Legendre expansion of the measured analyzing powers allows some direct conclusions without referring to the complete matrix-element fit. Following the nomenclature of Ad'yasevich [16] the coefficients $a_{zz}(1)$ and $a_{xz}(1)$ have a common term $D_{01}(0,1)$

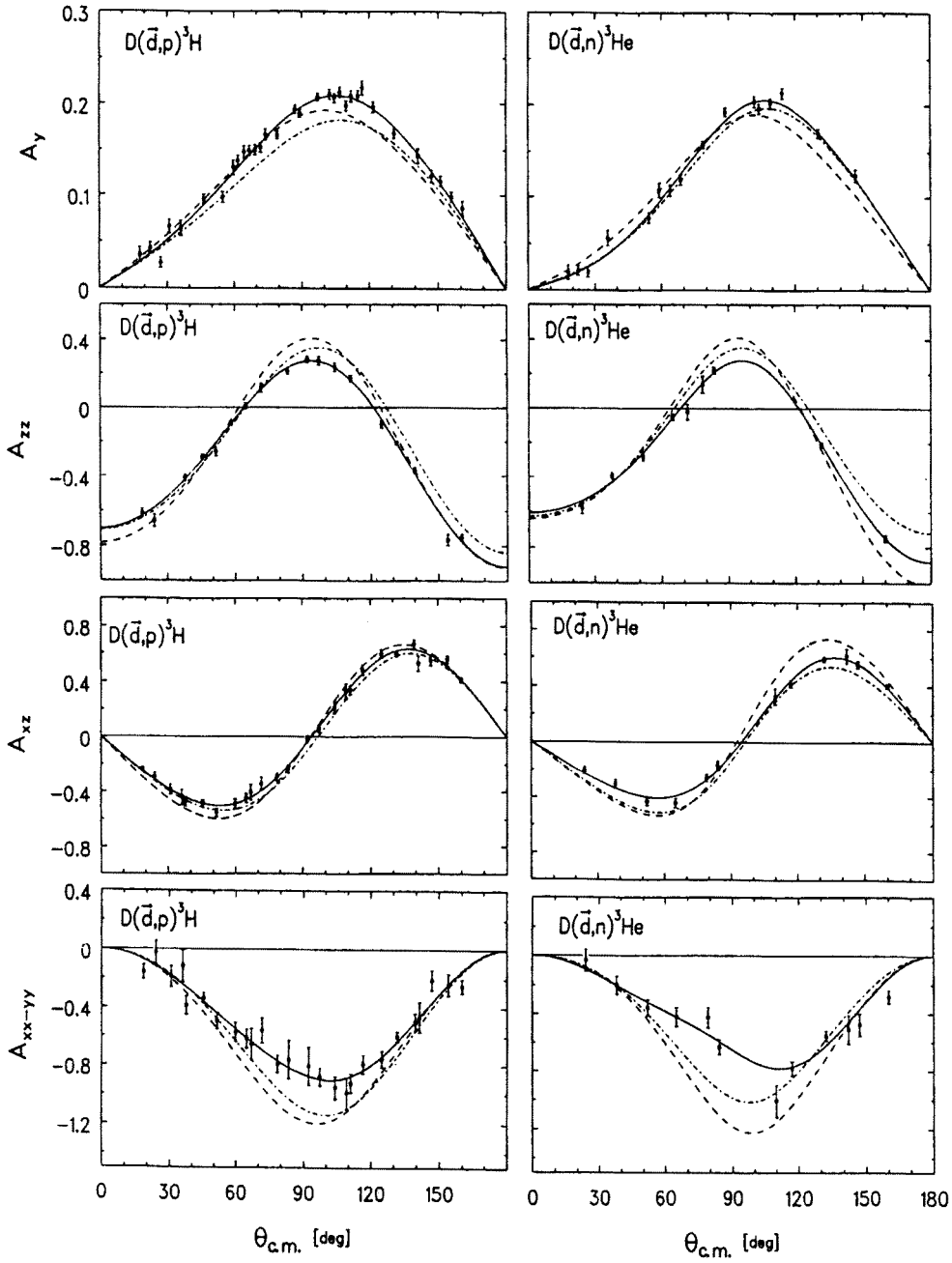

Fig. 1 : Measured analyzing powers of the D + D reactions at $E_{lab.} = 28 \pm 3$ keV
Solid lines : Legendre fit , dashed lines : R-matrix analysis by Hale [28],
dot-dashed lines : present matrix-element fit

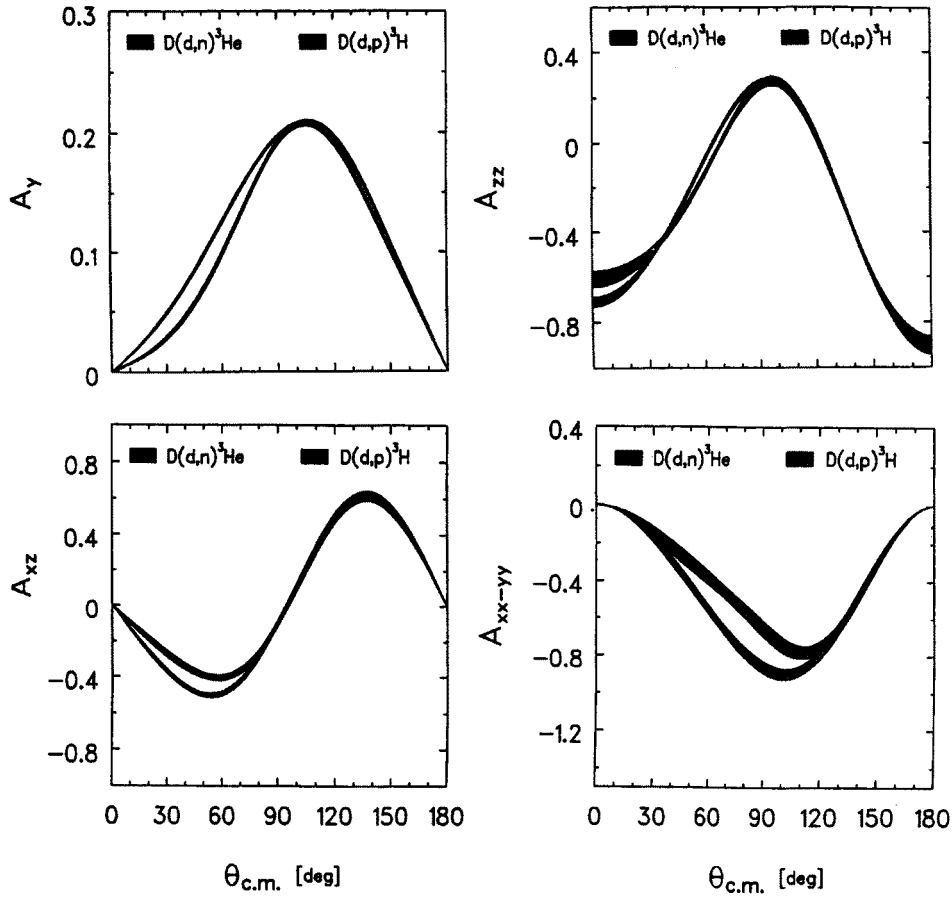

Fig. 2: Comparison of the Legendre-fit results for both reactions. The shaded areas are error bands from the covariance matrix of the fit

$a_{zz}(1) \sim D_{01}(0,1) + f_1$ where f_1 is some bilinear matrix-element combination, and

$a_{xz}(1) \sim D_{01}(0,1) + f_2$, where f_2 is some other combination, and

$$D_{01}(1,0) = c_{11}\mathrm{Re}(\beta_{11}\gamma_1^*) + c_{21}\mathrm{Re}(\alpha_{11}\delta_1^*) + c_{31}\mathrm{Re}(\alpha_{12}\delta_1^*) + c_{41}\mathrm{Re}(\alpha_3\delta_1^*)$$

c_{ij} are known constant factors. Experimentally $a_{zz}(1) \approx a_{xz}(1) \approx 0$. In a similar way the third expansion coefficients of the tensor analyzing powers are

$$a_{zz}(3) = k_1 D_{03}(0,1) + f_3$$

$$a_{xz}(3) = k_2 D_{03}(0,1) + f_4$$

$$a_{xx-yy}(3) = k_3 D_{03}(0,1) + f_5 \qquad \text{and}$$

$$D_{03}(0,1) = c_{13}\mathrm{Re}(\beta_{11}\gamma_1^*) + c_{23}\mathrm{Re}(\alpha_{11}\delta_1^*) + c_{33}\mathrm{Re}(\alpha_{12}\delta_1^*) + c_{43}\mathrm{Re}(\alpha_3\delta_1^*)$$

From this set of equations and the data on can calculate three values for $D_{03}(0,1)$:

0.202, 0.238 and 0.199 for the D(d,p)^{3}H reaction, and
0.312, 0.316 and 0.300 for the D(d,n)^{3}He reaction,

in good agreement and different from zero outside the errors. Possible conclusions to be drawn from both sets are : Quintet D-state (as all D-state) contributions are weak at this energy, whereas quintet S-state contributions must be substantial, since all matrix element products in $D_{03}(0,1)$ contain these matrix elements. Significant differences between both reactions are also visible.

Another qualitative conclusion which used to be drawn is no more possible. It concerns the large vector analyzing powers. Without quintet transitions this would indicate that triplet-singlet transitions (matrix element β_{11}) which appear in the expansion of $a_y(1)$ and which are forbidden to first order, do take place. Now also quintet S-waves in interference with P waves may be responsible for the large A_y.

6. MATRIX-ELEMENT ANALYSIS

The set of all data below 500 keV used in the former analyses [13] has been augmented by our new data and some other new data that became available recently [14,15] and again subjected to the matrix element fit procedure. An additional improvement consisted in choosing Coulomb function routines better suited for the very-low energy regime.

In this new matrix-element fit the interaction radius of the two deuterons - instead of fixing it to a conventional value as usual and as in the former analysis [13] - has been treated as a fit parameter The values obtained were R =2.36 ± 0.43 fm for the $D(d,n)^3He$ and R = 3.81 ± 0.20 fm for the $D(d,p)^3H$ reaction for minimum χ^2. It is interesting that both values come out differently indicating that probably the Coulomb repulsion between the deuteron and the proton in the case of the $D(d,p)^3H$ reaction allows the neutron to react at smaller distances than the proton in the $D(d,n)^3He$ case. The matrix-element results are again values of modulus and phase for all transitions for both reactions. Table 2 shows the new results for the moduli of the 16 "internal" matrix elements of both reactions.

Table 2

RESULTS OF THE MATRIX-ELEMENT ANALYSIS (MODULI OF $\hat{T}_{\alpha\beta}$)

(Errors in parentheses)

		$D(d,p)^3H$	$D(d,n)^3He$
Interaction radius	R(fm) :	3.81 (0.20)	2.36 (0.43)
Matrix element	α_0	3.59 (0.07)	6.18 (0.46)
	α_{10}	1.03 (0.42)	11.82 (5.97)
	β_{11}	5.41 (0.12)	8.68 (2.93)
	α_{11}	9.15 (0.44)	17.94 (1.35)
	α_{12}	1.47 (0.34)	7.26 (5.50)
	α_2	17.66 (1.09)	79.46 (43.07)
	β_2	5.82 (0.30)	15.00 (12.62)
	α_3	3.91 (0.23)	11.40 (2.50)
	γ_1	1.24 (0.07)	1.74 (0.16)
	γ_2	21.16 (2.81)	119.88 (44.24)
	γ_3	15.28 (2.23)	73.49 (39.86)
	δ_1	1.45 (0.01)	1.66 (0.60)
	δ_2	8.94 (2.52)	24.08 (8.20)
	δ_3	21.17 (2.82)	83.90 (64.48)
	δ_4	19.40 (3.64)	13.08 (13.19)
	δ_5	14.35 (1.92)	25.08 (24.44)

Figs. 3-7 on the following pages show the total cross sections and the Legendre expansion coefficients of the differential cross sections and of the four analyzing powers together with the fit results of the matrix-element analysis as a function of lab. energy. The figures give an impression of the quality of the fit, but also of the data situation, which prompted us to omit certain data sets from the analysis (They are indicated by an asterisk).

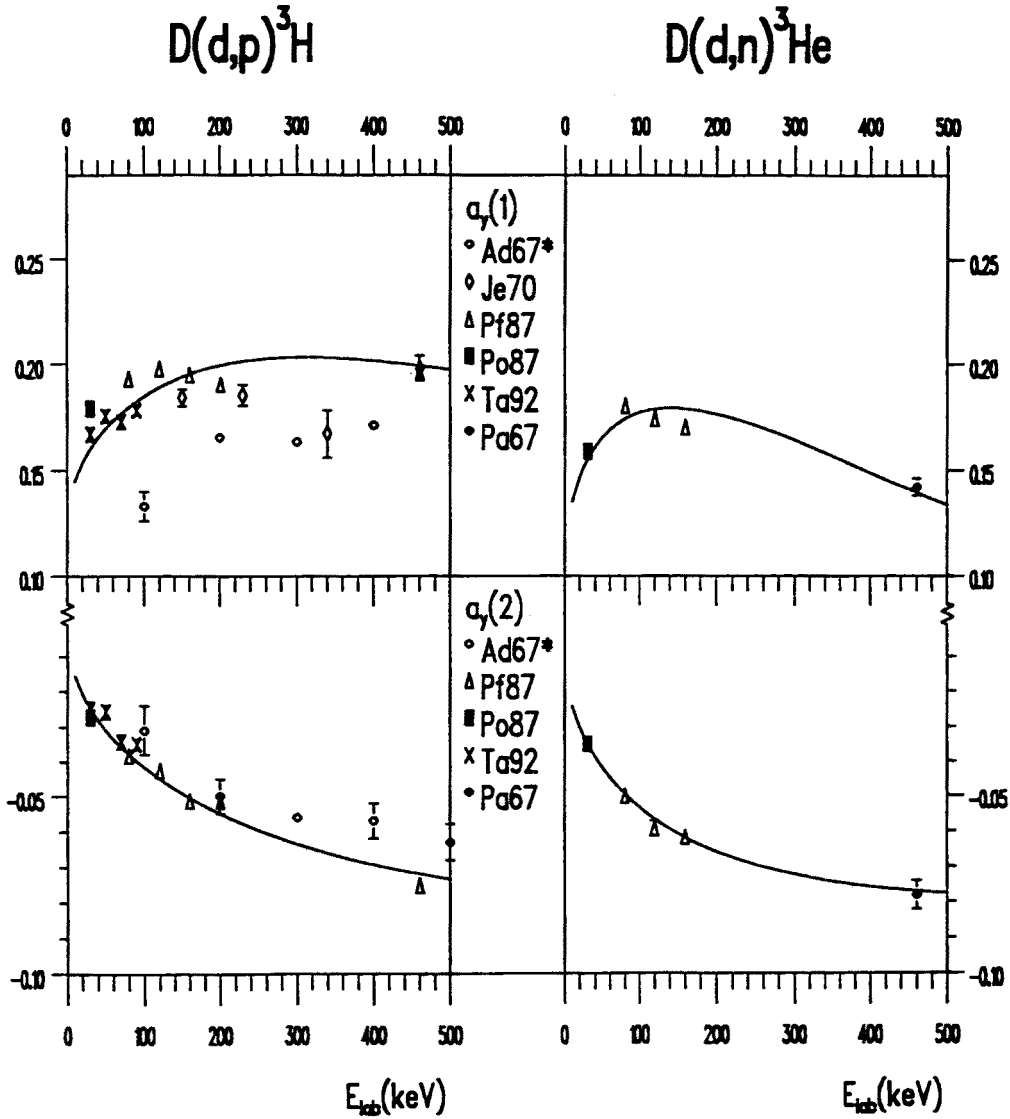

Fig. 3: Excitation functions of the expansion coefficients of the vector analyzing powers. The solid line is the result of the present matrix-element fit

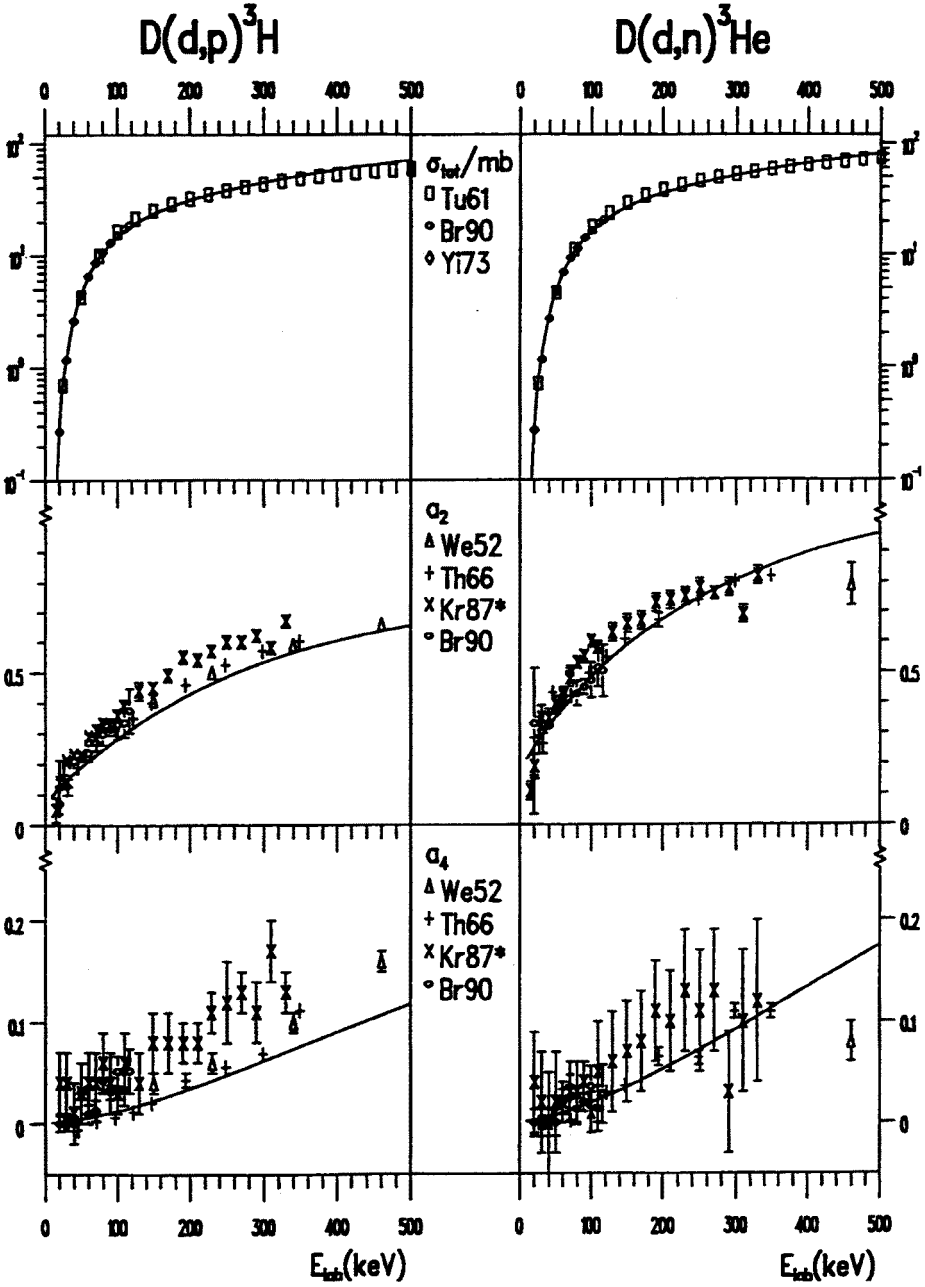

Fig. 4: Same as fig. 3, but for the total cross sections and the expansion coefficients of the differential cross sections

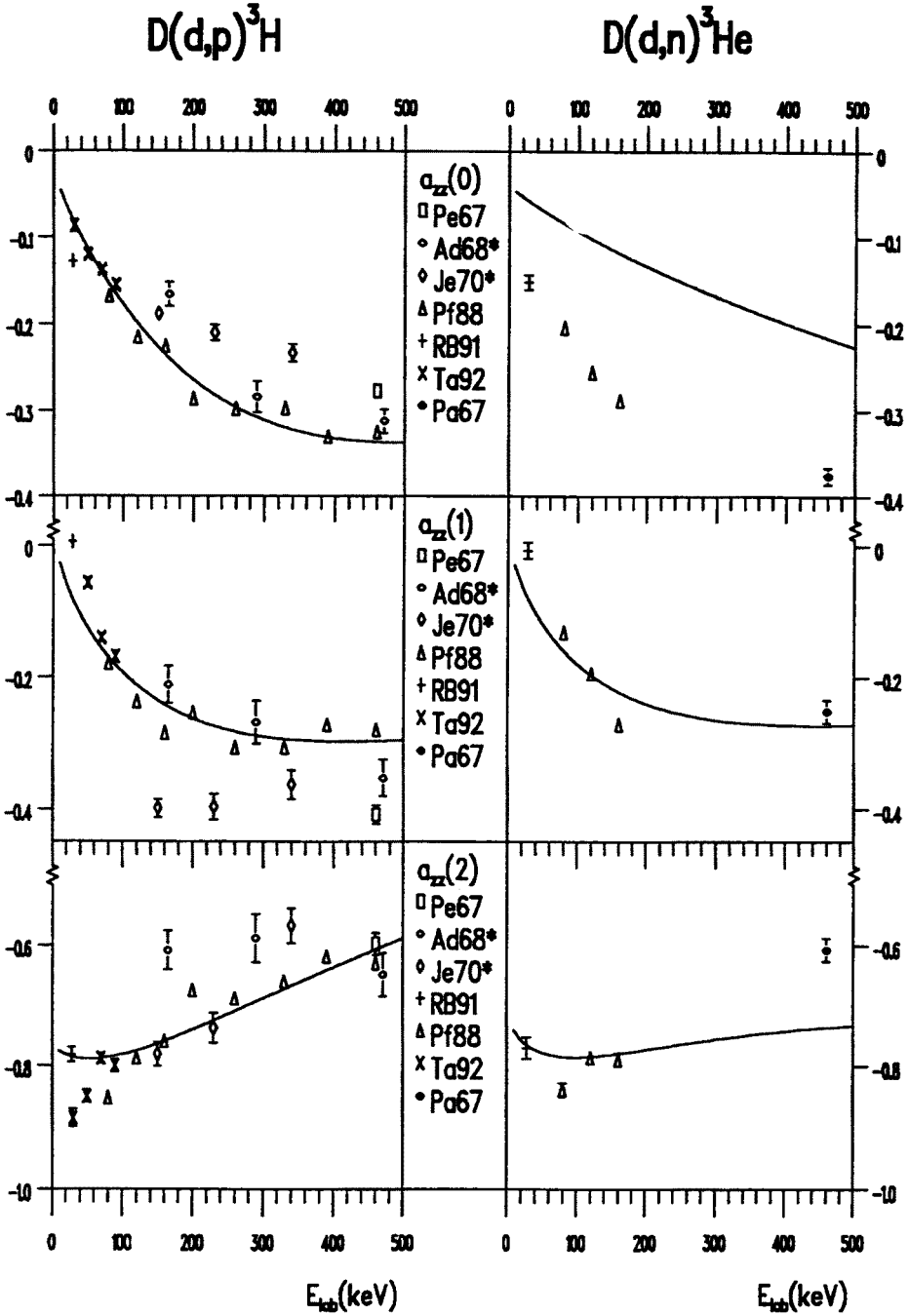

Fig. 5: Same as fig. 3, but for the tensor analyzing powers A_{zz}

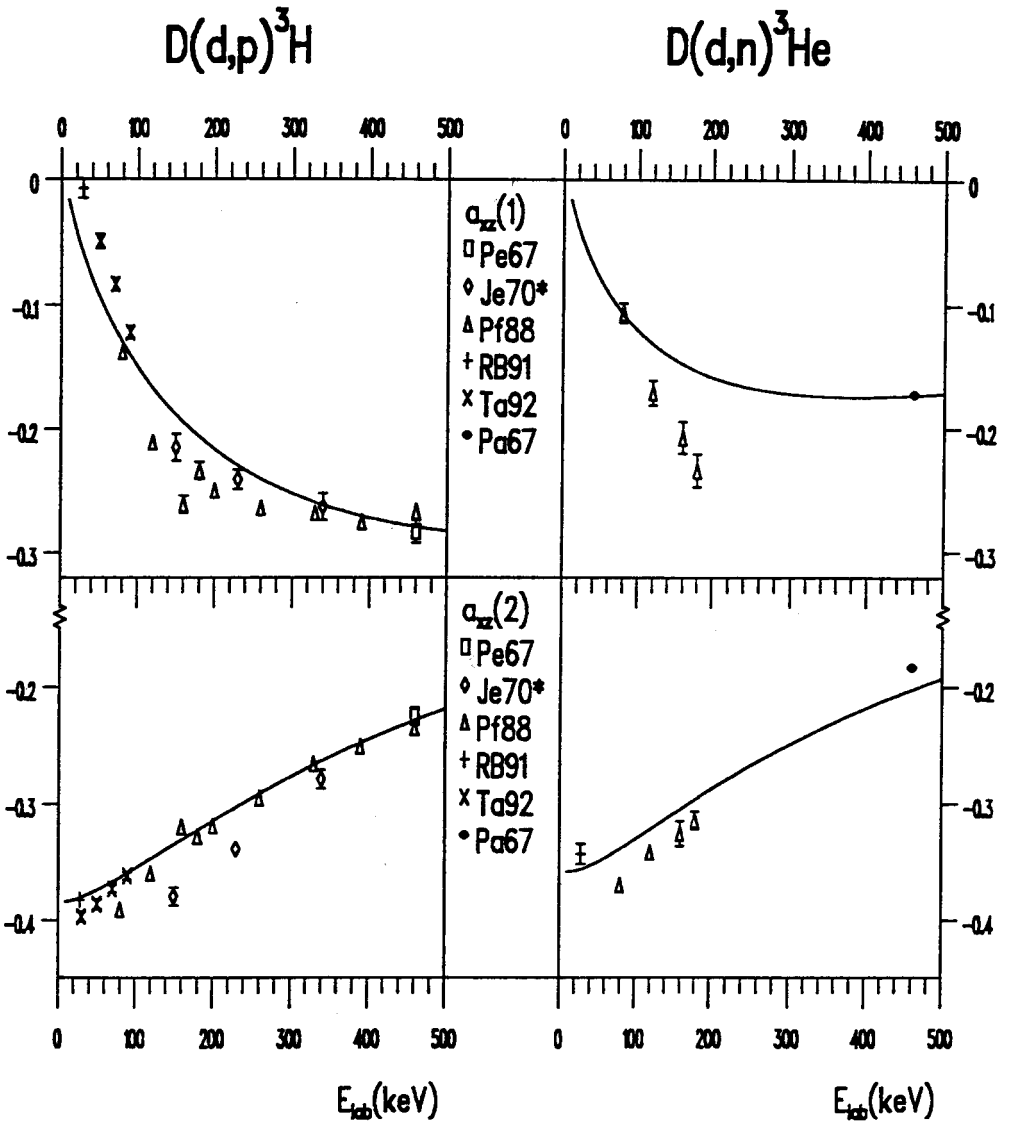

Fig. 6: Same as fig. 3, but for the tensor analyzing powers A_{xz}

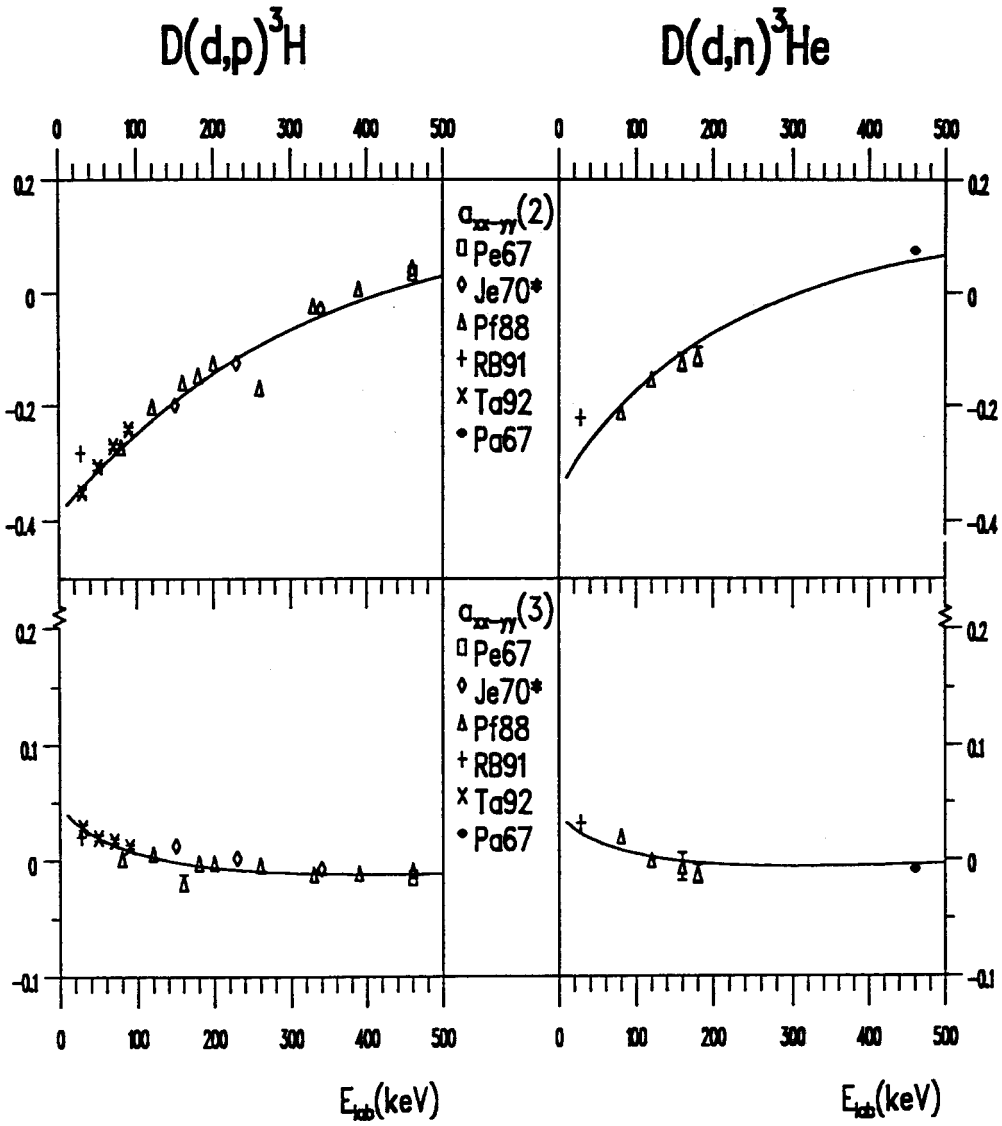

Fig. 7: Same as fig. 3, but for the tensor analyzing powers A_{xx}-A_{yy}

7. CONCLUSIONS

7.1. General conclusions

Due to the changes indicated, the results differ numerically somewhat from the former analysis [13], but qualitatively the conclusions drawn earlier do not change. They are :

- Quintet S-wave transitions are not suppressed, but contribute substantially to the reactions. From table 2 we learn that the two quintet S wave transitions are of the same order of magnitude as the singlet S wave transition for both reactions. They obviously proceed easily via the 2^+ intermediate state. Table 3 gives a comparison of the relevant new matrix-element ratios with an RRGM prediction and R-matrix analysis results, both cited from [32], and with our earlier results [13].

Table 3

COMPARISON OF S-WAVE MATRIX ELEMENT RATIOS AT $E_{c.m.}$ = 40 keV

	RRGM	R-matrix	Matrix-element fit	
			[13]	this work
$\lvert\gamma_1\rvert / \lvert\alpha_o\rvert$	0.24	0.92	0.43	0.28
$\lvert\delta_1\rvert / \lvert\alpha_o\rvert$	0.12	0.72	0.34	0.27
$\lvert\delta_1\rvert / \lvert\gamma_1\rvert$	2.0	1.28	1.27	0.95

- Table 2 shows that the contributions from the incoming quintet D waves, especially the $\langle {}^5D_0 \mid 0^+ \mid {}^1S_0 \rangle$ transition, are not negligible. However, one has to keep in mind that in the observables its effects appear suppressed by a rather small penetrability factor.

- Finally, the matrix element β_{11} discussed above qualitatively now turns out to be quite large. The assumption of many authors [12,30] that triplet-singlet transitions do not occur is therefore not justified and has to be explained by higher-order processes (e.g. a final state interaction [31]).

7.2. Polarized fusion

The sum rule for polarized correlation cross sections is given by:

$$\sigma_0 = 1/9\ (2\sigma_{1,1} + 4\sigma_{1,0} + 2\sigma_{1,-1} + \sigma_{0,0}) \qquad (15)$$

The indices (m,n) of the cross sections $\sigma_{m,n}$ denote the projections of the deuteron spins on the z axis which is in the direction of the initial momentum **k**. In our calculations which make use of the channel-spin representation it is not possible to distinguish $\sigma_{1,-1}$ from $\sigma_{0,0}$. In both cases the channel spin is $S_\alpha = 0$.

The calculation of the quintet polarization-correlation cross section using the earlier matrix-element results of [13] for the $D(d,n)^3He$ reaction showed not a suppression, but an enhancement over its purely statistical value. In figure 8 these results for the $D(d,n)^3He$ reaction are compared to results from the R-matrix analysis by Hale in [9] and especially for $\sigma_{1,1}$ to results from the DWBA calculation [6]. The $D(d,p)^3H$ reaction behaves quite similarly. The RRGM results of Hofmann and Fick for $\sigma_{1,1} / \sigma_0$ [12] coincide in fact with those of [9]. With the exception of the DWBA results the energy dependence of the polarized cross sections is similar to our results. This confirms the usefulness of penetrability functions which are used here exclusively to describe the energy dependence of the transitions amplitudes. However, for $\sigma_{1,1}$ a clear enhancement is found over the unpolarized one, even up to the resonance energy of 430 keV of the $^3\vec{He}(\vec{d},p)^4He$ reaction in contradiction to the DWBA calculations of [6].

Therefore the idea of a neutron-lean fusion reactor by using polarized fuel appears not to work. This behaviour can be explained only either by a second-order spin flip transition or an admixture of higher internal waves to the ground state of the nuclei involved which render possible a first order transition. In [7] where the authors came to the same conclusion concerning neutron suppression it was shown that the $S_\alpha = 2$ matrix elements are possible without any spin flip due to D-state admixtures in the deuteron.

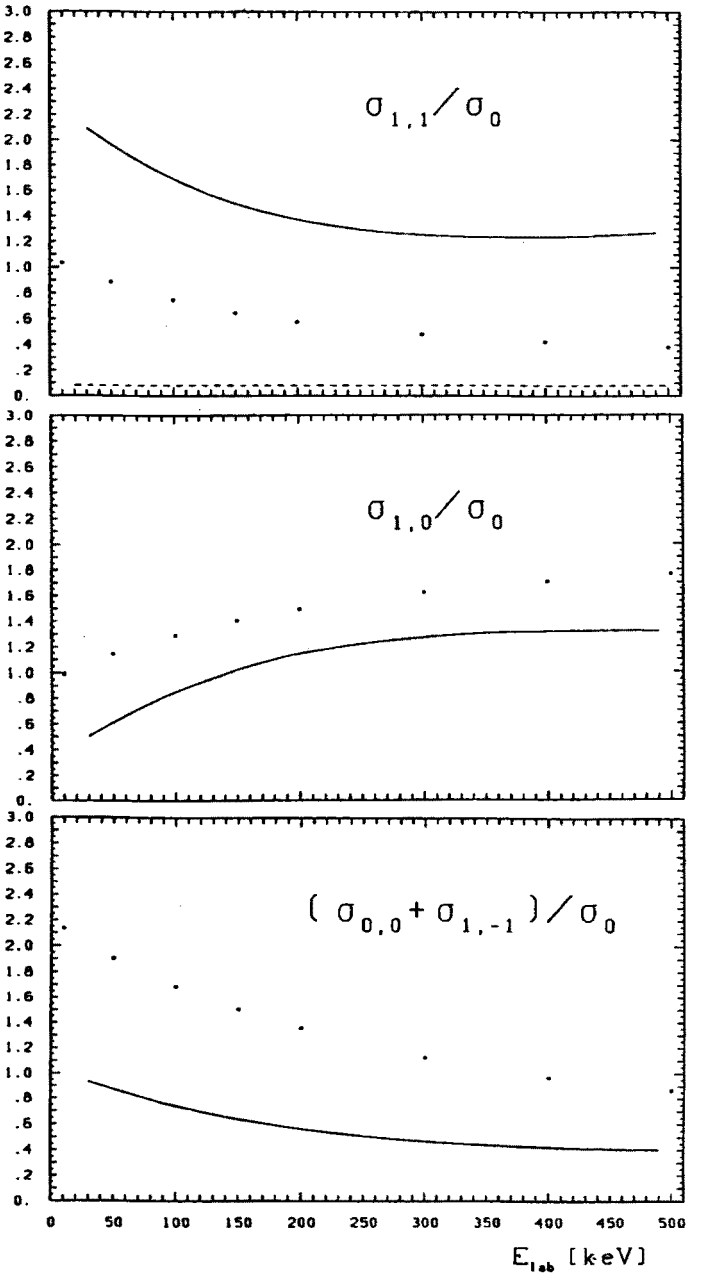

Fig. 8: Quintet-suppression factor (QSF) from the analysis [13], solid lines, compared to the RRGM (and R-matrix) results [9,12] : dots, and (for $\sigma_{1,1}$) to the DWBA prediction [6] : thin dashed line

With the results from table 2 all observables of the D+D reactions in the low-energy region < 500 keV may be calculated. Of particular interest are those which are not yet determined by experiment like polarization-transfer and polarization-correlation observables. Because of the multitude of such observables and the uncertainty whether they are accessible to experiment it is helpful to calculate them in order to support planning of future measurements. The figs. 9 and 10 show some results for spin-correlation and polarization-transfer observables in the form of contour plots obtained with the fit results from [13].

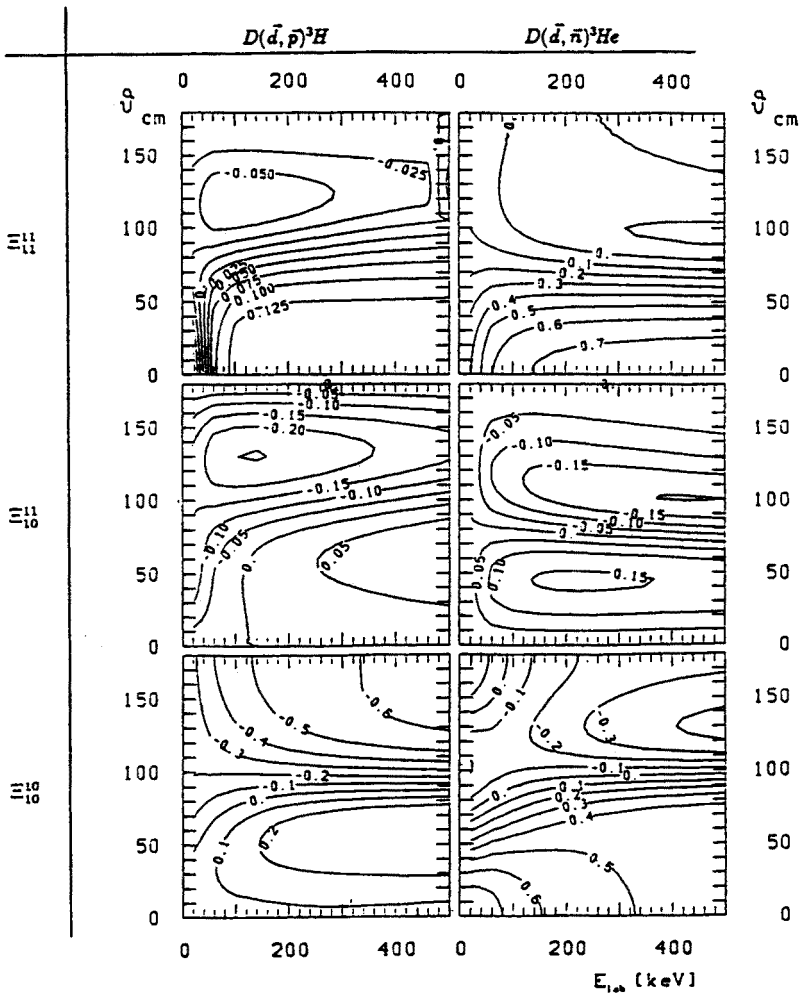

Fig. 9 : Contour plots of three polarization-transfer observables from [13]

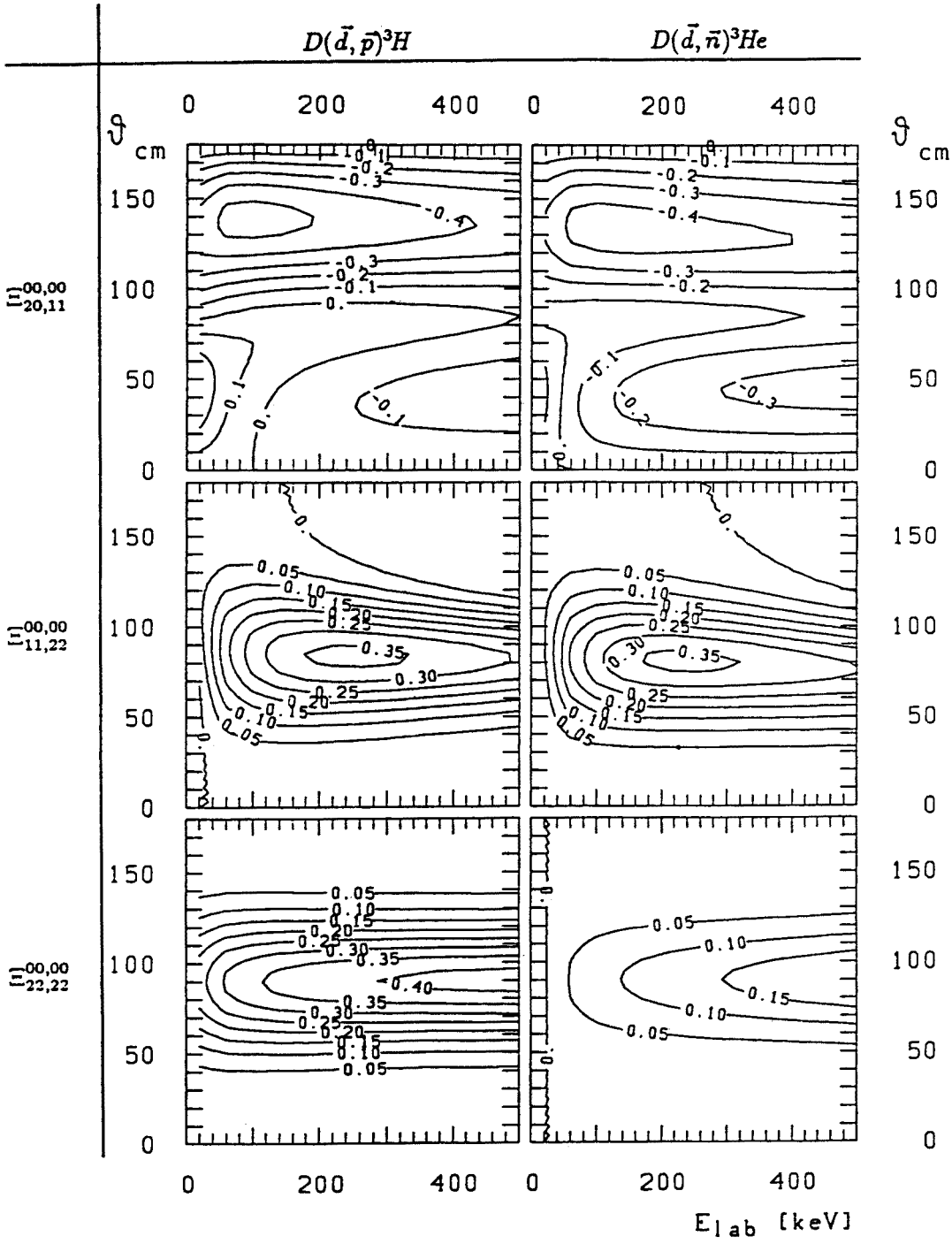

Fig. 10 : Contour plots of three polarization-correlation observables from [13]

ACKNOWLEDGMENTS

The author acknowledges contributions to the results presented here from many collaborators of the nuclear-reaction group. Thanks go to Prof. Clausnitzer and collaborators at Giessen for providing DPP targets and helping to make them, and again to the Giessen group and Dr. Tagishi for the permission to use their data in the matrix-element analysis prior to publication.

The work has been supported in part by BMFT, Bonn, under the contract numbers 06-OK-153 and 06-OK-272.

REFERENCES

1. Dolch, H.: Z. Phys. **100**, 401 (1936) and
Flügge, S.: Z. Physik **108**, 545 (1938)
2. Fermi, E., Amaldi, Phys. Rev . **50**, 899 (1936) and
Ladenburg, R., Kanner, M.H.: Phys. Rev . **52**, 911 (1937)
3. O. Yakubovsky, Sov. J. Nucl. Phys. **5**, 937 (1967)
P. Grassberger, W. Sandhas, Nucl. Phys. **B2**, 181(1967)
E.O. Alt, P. Grassberger, W. Sandhas, Phys. Rev. **C1**, 85 (1970)
4. Fonseca, A.C. : Phys. Rev. Lett. **63**,2036(1984); Phys. Rev. Lett. **55**, 1650 (1985); Phys. Rev. Lett. **63**, 2036(1989) ; Nucl. Phys. **A508**, 281c(1990)
5. Konopinski, E.J., Teller, E.: Phys. Rev. **73**, 822 (1948)
6. Zhang, J.S., Liu , K.F. , Shuy , F.W.: Phys. Rev. Lett. **55**, 1649 (1985); Phys. Rev. Lett. **57**, 1410 (1986)
7. Hofmann, H.M., Hale, G.M., Wölker , R.: Proc. Int. Workshop on Few-Body Approaches to Nuclear Reactions in Tandem and Cyclotron Energy Regions, Tokyo, 1986 (Oryu, S., Sawada, T., eds.), p. 162 Singapore : World Scientific 1987
8. Kulsrud, R.M., Furth, H.P., Valeo, E.J. , Goldhaber, M.: Phys. Rev . Lett. **49**, 1248 (1982);
Kulsrud, R.M.: Nucl. Instr. Meth. **A271**, 4 (1988);
9. Proc. Polarized Fusion Fuel Workshop , Madison, 1983, Report UWFDM-503, Univ . of Wisconsin, Madison, Wisc.
10. Ad'yasevich, B.P., Antonenko, V.G., Kuznetsov, D.A. : Sov. J. Nucl. Phys. **8**, 154 (1969)
11. Ad'yasevich ,B.P., Antonenko, V.G., Fomenko, D.E.: Sov.J. Nucl. Phys. **33**, 313 (1981)

12. Hofmann, H.M., Fick, D.: Phys. Rev. Lett. **62**, 2038 (1984); Phys. Rev. Lett. **55**, 1650 (1985)

13. Lemaitre, S.: Diplomarbeit, Universität Köln, 1989 ;
Lemaitre, S., Paetz gen. Schieck, H.: Few-Body Systems **9** (1990)155 ;
Proc. 7th. Int. Conf. on Polarization Phenomena in Nucl. Phys., Paris, 1990 (Boudard, A., Terrien, Y., eds.)p. 463. Colloque de Physique C6, Tome 51, Paris : Les Editions de Physique 1990

14. Krauss, A., Becker, H. W., Trautvetter, H. P., Rolfs, C., Brand, K.: Nucl. Phys. **A465**, 150 (1987);
Brown, R. E., Jarmie, N.: Phys. Rev. **C41**, 1391 (1990);
Pfaff, E.: Doktorarbeit Universität Giessen, 1989;
Pfaff, E., Kniest, N., Reiter, G., Clausnitzer, G.: Proc. Int. Conf. on Nucl Phys., Harrogate, 1986, Vol. 1 (IOP Conf. Series,Vol. 86),(Durell, J.L., Irvine, J.M., Morrison, G.C., eds.), p. 297 . Bristol: IOP 1987 ;
Proc. 6th Int. Symp. on Polarization Phenomena in Nucl. Phys., Osaka, 1985 (Kondo, M. et al., eds.) J. Phys. Soc. Jap. Suppl. **55**, 894 (1986)

15. Tagishi, Y., Nakamoto, N., Katoh, K., Togawa, J., Hisamune, T., Yoshida, T.: preprint, Phys. Rev. **C**

16. Ad'yasevich, B.P., Fomenko, D.E.: Soviet J. Nucl. Phys. **9**, 167 (1969)

17. Beiduk, F.M., Pruett, J.R., Konopinski, E.J.: Phys. Rev. **77**, 622 (1950);
Pruett, J.R., Beiduk, F.M., Konopinski, E.J.: Phys. Rev. **77**, 628 (1950)

18. Boersma, H.J.: Nucl. Phys. **A135**, 609 (1969)

19. Welton, T.A.: in : Fast-Neutron Physics, Vol. II , p. 1317. New York-London : Interscience , 1963

20. Heiss, P. : Z. Phys. **251** , 159 (1972)

21. Seiler,F.: Comp. Phys. Comm. **6**, 229 (1974);
Aulenkamp, H. : Diplomarbeit, Universität Köln, 1973;
G. Latzel, K.R. Nyga: priv. comm.
Hofmann, H. M. : priv. comm.

22. Blüge, G., Langanke, K.H., Plagge, M., Nyga, K.R., Paetz gen. Schieck, H.: Phys. Lett. **B 238**, 137 (1990)

23. Haeberli, W., Grüebler, W., Extermann, P., Schwandt, P.: Phys. Rev. Lett. **15**, 267 (1965)

24. Stevens, R.R., Ohlsen, G.G.: Proc. Third Int. Symp. on Polarization Phen. in Nucl. Reactions, Madison, 1970 (Barschall, H., Haeberli, W., eds.) p. 858. Madison: Univ. of Wisconsin Press 1971

25. Pfaff, E., Juritz, E.: Universität Giessen, private communication

26. Andersen, H.H., Ziegler, J.F.: Hydrogen Stopping Powers and Ranges in all Elements, Pergamon, 1977
27. Polke, B. : Diplomarbeit, Universität Köln, 1987;
Swillus, O. : Diplomarbeit, Universität Köln, 1990;
Randermann, R. : Diplomarbeit, Universität Köln, 1991;
Becker, B. : Diplomarbeit, Universität Köln, 1991
28. Hale, G.M. : priv. comm. (1991)
29. Wölker, R. : Doktorarbeit, Universität Erlangen/Nürnberg, 1987
30. Rook, J.R., Goldfarb, L.J.: Nucl. Phys. **27**, 79 (1961)
31. Liu, K.F. : priv. comm.
32. Gegner, Z.W.: Diplomarbeit, Universität Erlangen/Nürnberg, 1989